*Journal of the European Ceramic Society* **15** (1995) 51–55

0955-2219/95/$9.50

# Ionic Conductivity of Fully Stabilized $ZrO_2$ : MgO and Blocking Effects

Eliana N. S. Muccillo[a] & M. Kleitz[b]

[a] Instituto de Pesquisas Energéticas e Nucleares, Comissão Nacional de Energia Nuclear S. P., C.P. 11049-Pinheiros, 05422-970 Sao Paulo, S.P., Brazil
[b] Laboratoire d'Ionique et d'Electrochimie du Solide de l'INP de Grenoble, Associé au CNRS, BP 75, 38402 St. Martin d'Hères Cedex, France

(Received 23 February 1994; revised version received 1 June 1994; accepted 14 June 1994)

***Abstract***

*Ionic conductivity measurements were performed by impedance spectroscopy on $ZrO_2$–MgO 13·7 mol%, in the 270–700°C temperature range. The diagrams show characteristic intragrain and grain boundary semicircles. Activation energies for the intragrain conductivity and the intergrain blocking effect are 126 and 141 kJ mol$^{-1}$, respectively. The estimated specific conductivity is 9·8 S m$^{-1}$ at 1000°C. The conductivity blocking effect at the grain boundaries is very similar to that of yttria-stabilized zirconia.*

## 1 Introduction

There has been significant interest in zirconia-based ceramic materials for several applications. Some of them (SOFCs, oxygen sensors and pumps, etc.) are based on the high oxide ion conductivity of the so-called stabilized zirconias. The majority of the zirconias investigated for this property contain trivalent cations as stabilizers. They induce higher conductivities than the divalent cations.

Mg-doped zirconia solid solutions have received less attention because of an instability of the cubic phase that results in a gradual degradation of its properties. Over the last decade, it has been demonstrated that an aging treatment at 1100°C slows down the decomposition reaction and, simultaneously, improves the thermal shock resistance of partially stabilized zirconias.[1] This has prompted new investigations on this system, mostly focused on mechanical properties. So far, relatively few studies[2–6] have dealt with its electrical properties and, in most cases, the conductivities have been measured by DC techniques, with no attention given to the microstructure effects.

Muccillo[7] has examined the correlations between the phase decompositions and the electric properties of the system using impedance spectroscopy. This paper reports results on the cubic phase containing 13·7 mol% of MgO which can be regarded as a sort of reference. As in other zirconia systems, the conductivity of the $ZrO_2$–MgO cubic phase is predominantly ionic and oxide ions are the charge carriers. Reported conductivity values[2] at 1000°C lie between 0·82 and 4·0 S m$^{-1}$. The literature data[2] on the conduction activation energy present an unusually broad dispersion, ranging from 82 to 141 kJ mol$^{-1}$. From diffusion measurements[8] in the cubic phase, it has been found that the oxygen diffusion activation energy is 63 kJ mol$^{-1}$. That of the Mg–Zr interdiffusion[9] is 285 kJ mol$^{-1}$.

Impedance spectroscopy has been widely used for characterizing other zirconia-based materials.[3,5,10–12] It is capable of separating the specific electric response of the material, the so-called intragrain response, from that of the grain boundaries which is always characterized by an additional resistance.

## 2 Experimental

The starting materials were $ZrO_2$ (DK-2 type, Zirconia Sales) and MgO (analytical grade from Merck). The following analyses were carried out: Hf content by neutron activation, other metallic impurities by spectrographic analysis, surface area by BET, distribution of particle size by sedimentation and particle/agglomerate morphology by scanning electron microscopy.

Pellets (typically 0·95 cm in diameter and 0·16 cm high) were prepared by conventional ceramic processing involving wet mixing, pressing, sintering at 1650°C for 2 h and machining. The apparent

**Table 1.** Results of chemical and physical analyses performed on starting powders (S: surface area, Dp: mean particle/agglomerate size)

| | *Hf* (%) | *Fe* (ppm) | *Si* (ppm) | *Al* (ppm) | *Surface area (S)* ($m^2/g$) | *Mean particle/ agglomerate size (Dp)* ($\mu m$) |
|---|---|---|---|---|---|---|
| $ZrO_2$ | 1·30 | 15 | 400 | 100 | 3·4 | 2·5 |
| MgO | — | 50 | — | — | 34·5 | <0·2 |

density of the sintered specimens was determined by the hydrostatic method and their phase content by X-ray diffractometry. Microscopic examinations were done on polished and chemically etched or fractured surfaces. The Mg content was confirmed by neutron activation analysis, checking on possible MgO losses by surface evaporation.[13]

For electrical measurements, Pt and Ag electrodes were applied by painting. Silver electrodes have been found to give a much smaller interference between the material responses and the electrode characteristics, allowing a more accurate determination of the electric parameters. Impedance measurements were performed from 5 Hz to 13 MHz with a HP 4192A impedance analyzer, in the 270–700°C temperature range. Data were collected during heating and cooling cycles. The results were analyzed in the impedance mode, using a special computer program.[14]

## 3 Results and Discussion

The MgO content of all sintered samples was determined to be 13·7 mol%, and the diffractogram profiles only exhibited the cubic phase reflections.

Table 1 shows the results of the powder analyses. The main impurity is silicon, at a level normally found in most technical zirconia powders. The mean particle/agglomerate size (2·5 $\mu$m) obtained by sedimentation, was taken as usual as the value corresponding to 50 wt% of the particles finer than it.

The relative density of the sintered pellets was about 80%, due to a large closed porosity. Figure 1 is a typical micrograph of a fractured surface showing the extensive intragranular, intergranular and triple-point porosities. The average grain size determined from a polished and etched surface is about 18 $\mu$m.

To improve the mechanical characteristics of Mg-partially stabilized zirconias, it is common practice to sinter the material at a relatively high temperature ($T > 1800$°C) and subsequently to quench and then anneal it at a temperature slightly higher than that at which the eutectoid decomposition starts. This gives ceramics with an average grain size in the 50–100 $\mu$m range.[15] With sintering temperatures of about 1700°C, ceramics with average grain sizes of about 20 $\mu$m were obtained.[16] The present data on the fully stabilized solid solutions sintered at 1650°C agree with these last results.

A three-dimensional impedance plot obtained at 441°C is presented in Fig. 2. In the 300–600°C temperature range, all diagrams show the same features: a predominant high-frequency semicircle and a smaller low frequency semicircle (and part of the electrode response). As usual with zirconia-based solid electrolytes, the semicircle centers fall

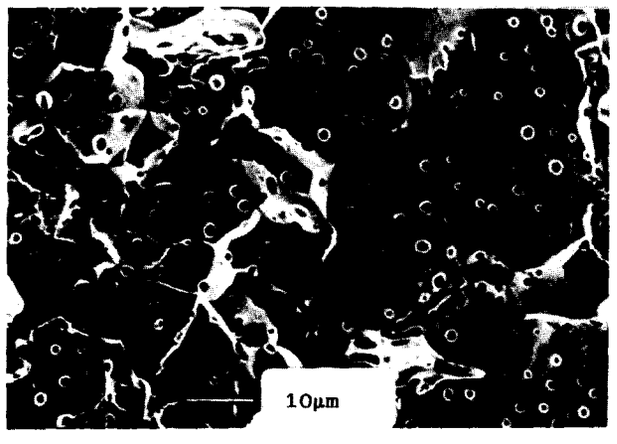


**Fig. 1.** Typical fracture surface of a $ZrO_2$–MgO 13·7 mol% sample sintered at 1650°C for 2 h.

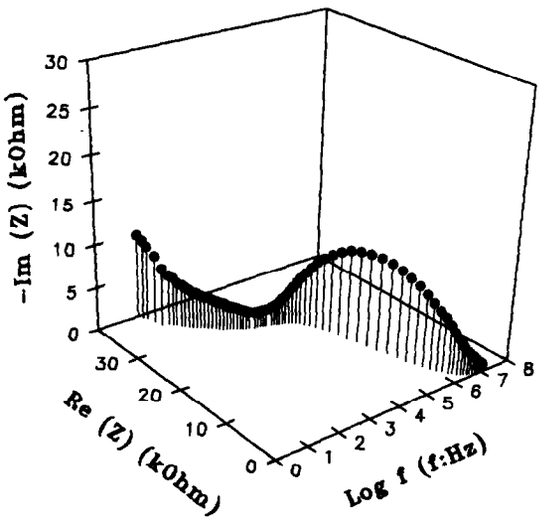


**Fig. 2.** Three-dimensional impedance plot recorded at 441°C (with Pt electrodes).

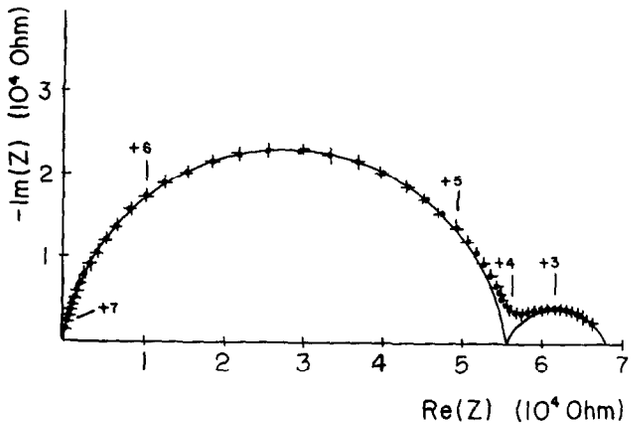


**Fig. 3.** Complex impedance plot recorded at 456°C (with Ag electrodes). The figures on the diagram indicate the decimal logarithms of the measuring frequencies.

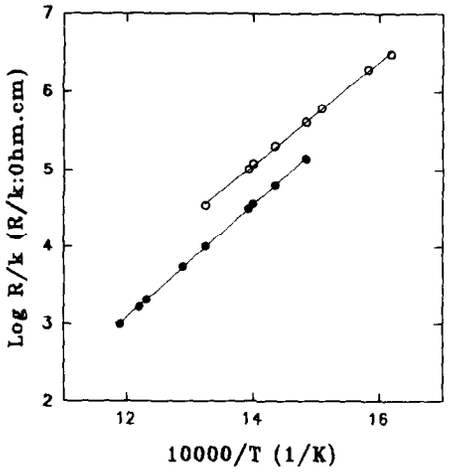


**Fig. 5.** Arrhenius diagram of the resistivities: (○) intragrain and (●) intergrain resistivities.

below the real axis. The off-axis angles are of the order of 12 and 18 degrees, respectively, for the high- and low-frequency semicircles. The high-frequency semicircle describes the intragrain resistance and capacitance relaxation. The low-frequency semicircle is related to conductivity blocking effects at grain boundaries. It is relatively small, because of a rather low grain boundary density (a rather high average grain size). In more conventional yttria-stabilized zirconias,[10] the relative magnitude of the grain boundary blocking effect is similar for a similar grain size. Details are given later in terms of a blocking factor.

Figure 3 presents an example of curve fitting performed on experimental data. Both intragrain and grain boundary contributions can be readily separated in this way in the temperature range 300–600°C. The data analysis was restricted to this temperature range where a reasonably good accuracy for the conductivity parameters was obtained.

Figure 4 shows the logarithms of the relaxation frequencies determined at the apex of the semi-

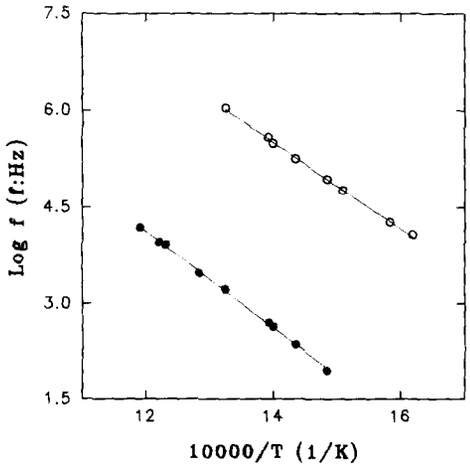


**Fig. 4.** Arrhenius diagram of the relaxation frequencies: (○) intragrain and (●) intergrain responses.

circles as functions of temperature. The fitted straight lines are approximately parallel. A similar observation was also made with zirconia–yttria ceramics.[11,12] At 400°C, the frequency ratio is equal to $1{\cdot}1 \times 10^{-3}$. It is very similar to the value ($0{\cdot}99 \times 10^{-3}$) quoted for an yttria-stabilized zirconia,[12] indicating similar average morphologies for the grain boundaries.

Values of the specific resistivities $R/k$ have been determined from the intersections of the impedance arcs with the real axis, $R$ being the resistances and $k$ the geometrical factors of the samples. Figure 5 shows the Arrhenius plots of the intragrain and intergrain resistivities. There is no noticeable change in the slope of the intragrain resistivity in the investigated temperature range. This is in contrast with common observations on yttria-stabilized zirconias, but in agreement with results obtained by DC techniques, where no change of the Arrhenius slope has been observed, at least up to 1000°C.[6,17]

Activation energies and pre-exponential factors are given in Table 2. As is frequent in zirconia-based ionic conductors,[11] the difference between the activation energies of the intragrain and intergrain resistivities is about 15 kJ $mol^{-1}$. From the intragrain parameters one can estimate, by extrapolation, an intragrain conductivity of 9·8 S $m^{-1}$ at 1000°C. At this temperature the blocking effect of charge carriers by grain boundaries is negligible, and hence intragrain and DC conductivities are the same. The conductivity value is slightly higher

**Table 2.** Activation energies *(E)* and pre-exponential factors *(A)* of the intragrain and intergrain resistivities

| | *Intragrain* | *Intergrain* |
|---|---|---|
| $E$ (kJ $mol^{-1}$) | 126 | 141 |
| $A$ ($10^{-7}$ Ω m) | 6·6 | 0·17 |

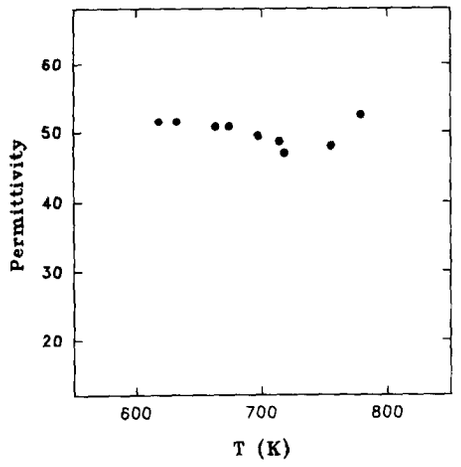


**Fig. 6.** Variation of the permittivity with temperature.

than reported data. This may be a consequence of different sintering conditions. It is well known that increasing the sintering temperature and sintering time greatly enhance the average grain size and modify the porosity. The grain size has no net effect on the bulk electrical characteristics, but porosity increases the intragrain resistivity.[11,18]

From the bulk semicircles a dielectric constant can also be calculated. As shown in Fig. 6, it does not vary much with temperature and is close to 50, a value similar to that (about 60) measured with yttria-stabilized zirconias under similar experimental conditions.[19]

Referring to a previous analysis by Dessemond and coworkers,[11,20] the blocking of the electric charge carriers at the grain boundaries by the blocking factor $\alpha_R$ can be defined by the equation:

$$\alpha_R = R_{\text{grain b.}}/(R_{\text{intrag.}} + R_{\text{grain b.}})$$

It measures the fraction of ionic carriers being blocked at grain boundaries. Over the rather narrow temperature range where it could accurately be determined, it is approximately independent of temperature (Fig. 7). Its average value is 0·24.

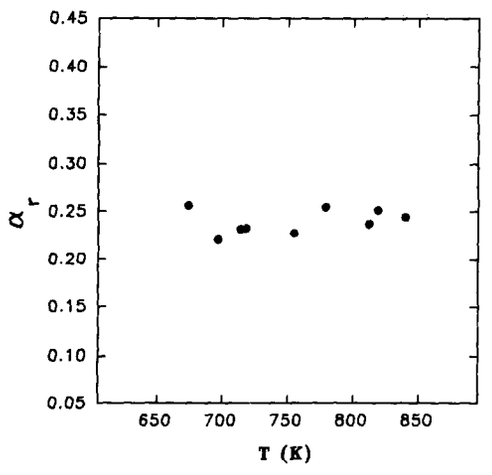


**Fig. 7.** Variation of the grain boundary blocking factor with temperature.

## 4 Conclusions

The main conclusions are:

—The impedance diagrams of fully stabilized $ZrO_2$–MgO ceramics prepared by solid-state synthesis present two well-resolved semicircles as for other cubic zirconia systems. The activation energies for the intragrain resistivity and the intergrain blocking effect are 126 and 141 kJ $mol^{-1}$, respectively.

—The estimated specific conductivity is 9·8 S $m^{-1}$ at 1000°C.

—The specific dielectric constant and the ion-blocking parameters are very similar to the equivalent parameters of yttria-stabilized zirconias.

## Acknowledgments

The authors acknowledge CNPq-RHAE for a scholarship to one of the authors (E.N.S.M.) and Zirconia Sales for providing the zirconia powder.

## References

1. Hannink, R. H. J. & Garvie, R. C., Sub-eutectoid aged Mg-PSZ alloy with enhanced thermal up-shock resistance. *J. Mater Sci.*, **17** (1982) 2637–43.
2. Etsell, T. H. & Flengas, S. N., The electrical properties of solid oxide electrolytes. *Chem. Rev.*, **70** (1970) 339–52.
3. Wen, T. L., Li, N. X., Kuo, C. & Weppner, W., Conductivity of MgO-doped $ZrO_2$. *Solid State Ionics*, **18/19** (1986) 715–9.
4. Poulsen, F. W., Sorensen, J. B. B., Ahari, K. G., Knab, G. G. & Hartmanova, M., Oxygen ion conduction in ternary zirconia mixtures: effect of SrO on MgSZ. *Solid State Ionics*, **40/41** (1990) 947–51.
5. An, S., Wu, X., Wu, W. & Lin, Q., Effect of heat treatment on structure and properties of MgO–PSZ electrolyte. *Solid State Ionics*, **57** (1992) 31–4.
6. Badwal, S. P. S., Zirconia-based solid electrolytes: microstructure, stability and ionic conductivity. *Solid State Ionics*, **52** (1992) 23–32.
7. Muccillo, E. N. S., Impedance spectroscopy and internal friction in $ZrO_2$ : MgO solid electrolytes, Thesis (in Portuguese), IPEN, Universidade de São Paulo, Brazil, 1993.
8. Ando, K., Oishi, Y., Koizumi, H. & Sakka, Y., Lattice defect and oxygen self-diffusion in MgO-stabilized $ZrO_2$. *J. Mater. Sci. Lett.*, **4** (1985) 176–80.
9. Sakka, Y., Oishi, Y. & Ando, K., Cation interdiffusion in polycrystalline fluorite-cubic MgO–$ZrO_2$. *Bull. Chem. Soc. Jpn*, **55** (1982) 420–2.
10. Kleitz, M., Bernard, H., Fernandez, E. & Schouler, E., Impedance spectroscopy and electrical resistance measurements on stabilized zirconia. In *Advances in Ceramics*, Vol. 3, *Science and Technology of Zirconia I*, ed. A. H. Heuer & L. W. Hobbs. American Ceramic Society, Columbus, OH, 1981, pp. 310–36.
11. Dessemond, L., Spectrocopie d'impédance des fissures dans la zircone cubique. Thesis, Polytechnic Institut, Grenoble, France, 1992.

12. Kleitz, M., Pescher, C. & Dessemond, L., Impedance spectroscopy of microstructure defects and cracks characterization. In *Zirconia V, Science and Technology of Zirconia*, ed. S. P. S. Badwal, M. J. Bannister & R. H. J. Hanninck. Technomic, Lancaster, UK, 1993, pp. 593–608.
13. Sakka, Y., Oishi, Y. & Ando, K., Enhancement of MgO evaporation from MgO-stabilized $ZrO_2$ by grain-boundary diffusion. *J. Am Ceram Soc.*, **69** (1986) 111–3.
14. Kleitz, M. & Kennedy, J. H., Resolution of multi-components impedance diagrams. In *Fast Ion Transport in Solids, Electrodes and Electrolytes*, ed. P. Vashishta, J. N. Mundy & G K. Shenoy. North-Holland, Amsterdam, 1979, pp. 185–8.
15. Subbarao, E. C., Zirconia, an overview. In *Advances in Ceramics*, Vol. 3, *Science and Technology of Zirconia I*, ed. A. H. Heuer & L. W. Hobbs. American Ceramic Society, Columbus, OH, 1981 pp. 1–24.
16. Krishnamoorthy, P. R., Ramaswamy, P. & Narayana, B. H., Microstructural developments in Mg–Ti–PSZ systems. *J. Mater. Sci.*, **27** (1992) 1016–22.
17. Guillou, M., Millet, J., Asquiedge, M., Busson, N., Jacquin, M. & Palous, S., Propriétés électriques des zircones contenant de la magnésie. *C. R. Acad. Sci. Paris*, **262** (1966) 616–19.
18. Bonanos, N., Steele, B. C. H. & Butler, E. P., Applications of impedance spectroscopy. In *Impedance Spectroscopy*, ed. J. R. Macdonald. Wiley, New York, 1987, pp. 191–237.
19. Steil, M. C., Thevenot, F., Dessemond, L. & Kleitz, M., Impedance spectroscopy analysis of conduction percolation in zirconia–alumina composites. In *Proc. 3rd European Ceramic Society Conference*, ed. P. Duran & J. F. Fernandez. Faenza Editrice Iberica S. L., San Vincente, Spain, 1993, pp. 271–80.
20. Dessemond, L., Muccillo, R., Henault, M. & Kleitz, M., Electric effects of voids and second phases in stabilized zirconia. *Appl. Phys.*, **A57** (1993) 57–60.